

Theoretical optimization of the conversion efficiency in a pump-enhanced singly resonant optical parametric oscillator

XIAOJUAN YAN^{1,*}, ZHIHANG ZHANG¹, XINKE XU¹, SHIJUN REN¹, WEIGUANG MA^{1,2}, WEI TAN³

¹College of Physics and Electronic Engineering, Shanxi University, Taiyuan 030006, China

²Institute of Laser Spectroscopy, State Key Laboratory of Quantum Optics and Quantum Optics Devices, Shanxi University, Taiyuan 030006, China

³School of Information Science and Engineering, Shandong University, Qingdao 266237, China

We describe the theoretical treatment of the pump-enhanced singly resonant optical parametric oscillator (OPO) in which pump and signal simultaneously resonate in the cavity. The research shows that the photon conversion efficiency of pump-enhanced singly resonant OPO is related to the reflectivity of input coupler and the incident power ratio. Under specific incident power ratio, the maximum photon conversion efficiency can be obtained in the region where impedance matching is met. Considering the pump linear loss of 0.9% in the ring cavity, the maximum value of photon conversion efficiency is 99.6% that is higher than singly resonant OPO.

(Received August 19, 2021; accepted February 10, 2022)

Keywords: Pump-enhanced singly resonant OPO, Conversion efficiency, Mid-infrared laser

1. Introduction

The 3~5 μm mid-infrared laser has little attenuation when it travels through the atmosphere and is the infrared window of atmosphere. Moreover, this band covers the absorption peaks of many atoms and molecules. Therefore, the mid-infrared laser in this band has vital application value and prospect in many fields such as remote sensing [1], medical and health [2], spectroscopic analysis [3], military countermeasures [4], optical communication [5] and so on. The Optical Parametric Oscillator (OPO) is an important means to achieve the output of 3-5 μm infrared laser [6-12].

The OPO can be divided into two types: the singly resonant OPO in which only signal beams resonate in the cavity and the doubly resonant OPO in which both signal and idler beams resonate in the cavity. The singly resonant OPO has a higher threshold, but it has better stability and a wider tuning range than doubly resonant OPO, so it is often used to produce tunable mid-infrared laser. Theoretical researches show that under the plane wave approximation, when the linear losses of the pump are neglect and the ratio of incident pump intensity to threshold pump intensity (defined as incident intensity ratio) reaches 2.46, the pump can be fully converted in singly resonant OPO [13]. In fact, the laser (including pump, signal and idler) is a Gaussian spatial profile rather than a plane wave. Owing to the uneven intensity

distribution of Gaussian beam, the photon conversion efficiency is also spatially non-uniform and the maximum photon conversion efficiency cannot reach 100%, which is quite different from the result under the plane wave approximation. Recent many experimental studies have proved this conclusion [14-17]. In 2018, Shukla *et al.* presented a mid-infrared singly resonant OPO by using MgO:PPLN crystal pumped by a Yb fiber laser. The OPO yielded a maximum power of 2W at 3895 nm when incident pump power is 16 W, the photon conversion efficiency is about 37.5% [16]. In 2019, Sukeert *et al.* reported a green-pumped OPO based on periodically poled MgO-doped congruent lithium tantalate (MgO:cPPLT) by using a fan-out grating structure [17]. The OPO generates 131 mW of average idler power at 1476.5 nm for an input pump power of 1.8 W and photon conversion efficiency is about 20%.

On the basis of singly resonant OPO, the pump-enhanced singly resonant OPO has been developed historically in order to reduce the threshold pump power [18-22]. In 1994, G. Robertson *et al.* reported a pump-enhanced singly resonant type II LiB₃O₅ OPO pumped by a single-frequency argon-ion laser [18]. For 3.4 W of pump power, single-frequency output power of 500 mW in the non-resonant wave is obtained. In 1998, D. Chen *et al.* reported a low-threshold stable single-frequency continuous-wave OPO [20]. Tunable idler output up to 450 mW was obtained near 3 μm by

resonating both the signal wave and a single-frequency 1.06 μm Nd: YAG pump laser in a periodically poled lithium niobate OPO ring resonator. In addition to experimental research, the theory of pump-enhanced singly resonant OPO has also been studied in detail in Ref. [22]. Besides lowering the threshold, the pump-enhanced singly resonant OPO also can effectively improve the pump photon conversion efficiency. In this paper, we mainly focus on the theoretical optimization of conversion efficiency in a pump-enhanced singly resonant OPO in the case of Gaussian beam.

In Section 2, we first theoretically study the relationship between the incident intensity ratio and the pump photon conversion efficiency under the conditions of plane wave approximation and Gaussian beam for singly resonant OPO, and then establish the theoretical model of the pump-enhanced singly resonant OPO based on Gaussian beam. In Section 3, the variations of parameters including the intracavity photon conversion efficiency of the pump, the cavity-enhanced photon conversion efficiency of the pump, the signal and idler extraction efficiency, signal and idler output power with the changes of the incident pump power ratio and input coupler reflectivity are analyzed in detail. The optimal reflectivity of input coupler corresponding to the high-efficiency conversion region is obtained under different pump power ratio. Such theoretical treatment will provide a useful reference for researchers who design and develop an OPO device.

2. Theoretical analysis

The theoretical scheme is shown in Fig. 1, in which the signal at 1.4 μm and the mid-infrared idler at 3.8 μm are generated by a non-degenerate OPO pumped by a 1064 nm laser. The nonlinear crystal is a MgO:PPLN crystal with both ends anti-reflection coated for pump, signal and idler. The OPO cavity is a bowtie-shaped ring cavity with two plane mirrors M1 and M2 and two concave mirrors M3 and M4, where the M3 mirror is an input coupler for the pump, the M2 and M4 mirrors serve as the output couplers of the signal and idler, respectively. If the system is a singly resonant oscillator configuration for the signal, the cavity mirrors M1, M3, and M4 are highly reflecting for the signal and the output coupler M2 is partial transmission coated for the signal. The pump singly passes through the crystal and is transmitted from the mirror M4 together with the generated idler. If the system is a pump-enhanced singly resonant oscillator configuration, on the basis of the above, the mirrors M1, M2, and M4 also have high reflectivity at the pump and the input coupler M3 has partial transmission at the pump so as to fulfill the condition of impedance matching. The generated idler is still directly transmitted from the mirror M4. The frequency locking system is employed to lock the frequency of the pump laser to the cavity.

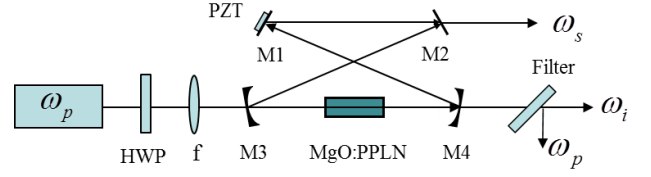


Fig. 1. Scheme diagram of OPO based on MgO:PPLN crystal in a bowtie-shaped ring cavity M1-M4, cavity mirrors; HWP, half wave plate; f, lens; PZT, piezo-electric transducer

2.1. The photon conversion efficiency of singly resonant OPO

2.1.1. Plane wave approximation

It is assumed that pump, signal and idler are all monochromatic plane waves. Ignore nonlinear effects above the third order, the coupled wave equations in a nonlinear crystal can be expressed as

$$\frac{dA_s^*}{dz} = -iB_s A_p^* A_i \exp[i(\Delta kz + \varphi)], \quad (1a)$$

$$\frac{dA_i}{dz} = iB_i A_p A_s^* \exp[-i(\Delta kz + \varphi)], \quad (1b)$$

$$\frac{dA_p}{dz} = iB_p A_s A_i \exp[i(\Delta kz + \varphi)], \quad (1c)$$

where the subscripts s , i , p represent respectively the signal, idler and pump, A is the complex amplitude of the light field, $B = d_Q \omega / (2nc)$, ω is the circular frequency of the light field, n is refractive index of the nonlinear crystal, c is the speed of light in vacuum, and d_Q represents the effective nonlinear coefficient of periodically poled crystal. For a first-order quasi-phase matched periodically poled crystal, $d_Q = 2d_{\text{eff}} / \pi$. The phase mismatch $\Delta k = k_s + k_i - k_p$ and the initial phase difference $\varphi = \varphi_s + \varphi_i - \varphi_p$.

By solving the coupled wave equations under the small signal approximation and considering the conditions of phase matching and signal resonance, the threshold pump intensity of singly resonant OPO can be approximated by

$$I_p^{\text{th}} = \frac{4cn_p n_s n_i (1 - r_s)}{\mu_0 \omega_s \omega_i d_Q^2 l^2 r_s}, \quad (2)$$

where r_s is the signal transmission coefficient in a round trip which includes the transmission losses of cavity mirrors and the linear losses of the crystal, l is the length of the crystal.

By solving the coupled wave equations of the signal resonance and considering the conditions of phase matching. The idler intensity at the output end face of the crystal can be written as

$$I_i(l) = \frac{\omega_i}{\omega_p} I_p(0) \sin^2(\Gamma l), \quad (3)$$

where Γ is the gain coefficient, $\Gamma^2 = B_i B_p |A_s(0)|^2$.

The photon conversion efficiency of singly resonant OPO can be defined as

$$\eta = \frac{\omega_p}{\omega_i} \frac{I_i(l)}{I_p(0)}. \quad (4)$$

Substituting Eq. (3) into Eq. (4), the photon conversion efficiency of the pump can be written as

$$\eta = \sin^2(\Gamma l). \quad (5)$$

According to Menley-Rowe relations, the increased number of signal photons is the same as the increased number of idler photons in the nonlinear process, so the increased signal intensity is as follows:

$$\Delta I_s = \frac{\omega_s}{\omega_i} I_i(l) = \frac{\omega_s}{\omega_p} I_p(0) \sin^2(\Gamma l). \quad (6)$$

When singly resonant OPO works in a steady state, the signal field in the cavity is constant, so the increased signal intensity in a single pass is output and lost by the cavity mirror and crystal, i.e.

$$\Delta I_s = I_s(0)(1 - r_s^2). \quad (7)$$

Substituting Eq. (6) into Eq. (7) and considering $r_s > 0.95$ in general case, we can get the following formula:

$$I_p(0) \approx I_p^{th} r_s \frac{(\Gamma l)^2}{\sin^2(\Gamma l)}. \quad (8)$$

So, the ratio of incident pump intensity to threshold pump intensity (defined as incident intensity ratio) now can be expressed as

$$I_{ratio} = \frac{I_p(0)}{I_p^{th}} = r_s \frac{(\Gamma l)^2}{\sin^2(\Gamma l)}. \quad (9)$$

The relationship between I_{ratio} and η is obtained by comparing Eq. (5) and Eq. (9), which can be written as

$$I_{ratio} = r_s \frac{(\arcsin(\sqrt{\eta}))^2}{\eta}. \quad (10)$$

2.1.2. Gaussian beam

The laser is a Gaussian spatial profile rather than a plane wave, so the results of plane wave approximation are not consistent with the experimental results. Boyd and Kleinman extend the results of plane wave to Gaussian beam [23]. When the crystal length is far less than the Rayleigh length of the pump in the cavity, i.e.

$l \ll \pi w_p^2 / \lambda_p$, where w_p is waist radius of the pump

Gaussian beam, the pump wave can be approximately regarded as a plane wave with amplitude distribution of $\exp(-r^2/w_p^2)$ in the cross section based on the near-field approximation. Thus, the pump intensity in the cross section can be expressed as

$$I_p(r) = I_p \exp(-2r^2/w_p^2), \quad (11)$$

where I_p is the central intensity of pump Gaussian beam.

The incident intensity ratio in the cross section now can be expressed as

$$I_{ratio}(r) = \frac{I_p \exp(-2r^2/w_p^2)}{I_p^{th}} = r_s \frac{(\Gamma l)^2}{\sin^2(\Gamma l)}. \quad (12)$$

Therefore, the photon conversion efficiency of the pump can be obtained by integrating in the cross section, i.e.

$$\eta_G = \frac{\int_0^{r_0} \sin^2(\Gamma l) I_p \exp(-2r^2/w_p^2) 2\pi r dr}{\int_0^\infty I_p \exp(-2r^2/w_p^2) 2\pi r dr}. \quad (13)$$

In the above equation, r_0 is the beam radius where the intensity is equivalent to threshold intensity, i.e.

$$r_0^2 = \frac{1}{2} w_p^2 \ln(I_p / I_p^{th}).$$

2.2. The photon conversion efficiency of pump-enhanced singly resonant OPO

The pump also resonates in the pump-enhanced singly resonant OPO so that the pump power can be amplified. The enhancement factor is defined as the ratio of the

resonant pump power in the cavity $P_{c,p}$ to the incident pump power $P_{in,p}$. According to Ref. [24, 25], it can be written as

$$E_p = \frac{P_{c,p}}{P_{in,p}} = \frac{1 - R_{in,p}}{\left[1 - \sqrt{R_{in,p}(1 - \delta_p)(1 - \eta_G)}\right]^2}, \quad (14)$$

where $R_{in,p}$ is reflectivity of the input coupler M3 for the pump, δ_p is the linear single-pass loss of the cavity (excluding the losses of the input coupler), η_G is the photon conversion efficiency of intracavity pump Gaussian beam and is shown in Eq. (13). According to the relation between power and intensity, the enhancement factor can be rewritten as follows:

$$E_p = \frac{P_{c,p}}{P_{in,p}} = \frac{P_{ratio}^{c,p}}{P_{ratio}^{in,p}} = \frac{I_{c,p}/I_p^{th}}{I_{in,p}/I_p^{th}} = \frac{1 - R_{in,p}}{\left(1 - \sqrt{R_{in,p}(1 - \delta_p)(1 - \eta_G)}\right)^2}, \quad (15)$$

where $I_{c,p}$ and $I_{in,p}$ are the central intensity of intracavity pump Gaussian beam and incident pump Gaussian beam, respectively, $P_{ratio}^{c,p}$ and $P_{ratio}^{in,p}$ are the ratio of intracavity pump power to threshold pump power (defined as intracavity power ratio) and the ratio of incident pump power to threshold pump power (defined as incident power ratio), respectively. When $R_{in,p}$, $P_{ratio}^{in,p}$, δ_p are set, the intracavity power ratio $P_{ratio}^{c,p}$ and the intracavity photon conversion efficiency η_G can be derived by solving Eqs.(12)-(13) and Eq.(15). Therefore, the generated signal and idler power by optical parametric oscillation can be estimated from:

$$\Delta P_s = \frac{\omega_s}{\omega_p} P_{c,p} \eta_G = \frac{\omega_s}{\omega_p} P_p^{th} P_{ratio}^{in,p} E_p \eta_G, \quad (16)$$

$$P_i = \frac{\omega_i}{\omega_p} P_{c,p} \eta_G = \frac{\omega_i}{\omega_p} P_p^{th} P_{ratio}^{in,p} E_p \eta_G. \quad (17)$$

Moreover, because the pump power is amplified by E_p , the cavity-enhanced photon conversion efficiency can be estimated as

$$\eta_G^{ce} = \frac{P_i/\omega_i}{P_{in,p}/\omega_p} = E_p \eta_G. \quad (18)$$

The condition for maximum η_G^{ce} can be obtained by equalizing the first derivative of Eq. (18) with respect to η_G to zero, which gives the condition that $\eta_G = 1 - (1 - \delta_p) R_{in,p}$. The linear loss δ_p is much smaller than 1 under normal conditions, whereby it can be neglected. This implies that the photon conversion efficiency of intracavity pump Gaussian beam η_G is equal to transmittance of input coupler M3 for the pump, which can be seen as an impedance matching condition.

2.3. The extraction efficiency of singly resonant OPO and pump-enhanced singly resonant OPO

In reality, whether singly resonant OPO or pump-enhanced singly resonant OPO, there are linear losses of resonant signal in the bowtie-shaped ring cavity. If the transmittance of output coupler M2 for the signal is T_s , and the other linear loss in a round trip for the signal is V_s , where $r_s^2 = 1 - (T_s + V_s)$, the actual output signal power from the output coupler M2 is

$$P_{out,s} = T_s P_s = \frac{T_s}{T_s + V_s} \Delta P_s. \quad (19)$$

The signal extraction efficiency of singly resonant OPO and pump-enhanced singly resonant OPO can be defined separately as

$$\eta_{out,s} = \frac{P_{out,s}/\omega_s}{P_{in,p}/\omega_p} = \frac{T_s}{T_s + V_s} \eta_G. \quad (20)$$

$$\eta_{out,s}^{ce} = \frac{P_{out,s}/\omega_s}{P_{in,p}/\omega_p} = \frac{T_s}{T_s + V_s} \eta_G^{ce}. \quad (21)$$

where $\eta_{es} = T_s/(T_s + V_s)$ is the escape efficiency of the resonator. The greater the escape efficiency, the higher the

signal output power and signal extraction efficiency. Therefore, in the actual operation, it is necessary to make V_s much smaller than T_s .

If the transmittance of output coupler M4 for the non-resonant idler is T_i , the actual output idler power is

$$P_{out,i} = T_i P_i. \quad (22)$$

The idler extraction efficiency of singly resonant OPO and pump-enhanced singly resonant OPO can be defined separately as

$$\eta_{out,i} = \frac{P_{out,i}/\omega_i}{P_{in,p}/\omega_p} = T_i \eta_G. \quad (23)$$

$$\eta_{out,i}^{ce} = \frac{P_{out,i}/\omega_i}{P_{in,p}/\omega_p} = T_i \eta_G^{ce}. \quad (24)$$

The extraction efficiency of idler is only affected by the transmittance of output coupler M4, because the idler is non-resonant. Moreover, the cavity mirror M4 is anti-reflection for the idler, so the extraction efficiency of idler is much greater than the extraction efficiency of the resonant signal. The band required in actual applications should be set to non-resonant.

3. Numerical simulation

In the following numerical simulation, it was assumed that the length of MgO:PPLN crystal is 50mm, the effective nonlinear coefficient d_{33} is 27×10^{-12} pm/V, the reflectivity of output coupler M2 is 98.5% at 1.4 μ m signal wave and the reflectivity of the other cavity mirrors at 1.4 μ m is 99.8%, the linear loss of nonlinear crystal for the signal is 0.1%, the threshold pump power is 760 mW based on a given set of reflectivities.

3.1. Comparison of photon conversion efficiency of singly resonant OPO based on plane wave approximation and Gaussian beam

By numerical simulation of Eqs. (10), (12) and (13), the plot of the pump photon conversion efficiency of singly resonant OPO as a function of incident intensity ratio I_{ratio} is shown in Fig. 2, where the red line and the black line represent the results obtained under the plane wave approximation and Gaussian beam conditions, respectively. It can be seen from this figure that the both pump photon conversion efficiencies show a trend with first an increasing and then a decreasing dependence on I_{ratio} . Under the plane wave approximation condition, when I_{ratio} reaches 2.46, the maximum η can reach 100%. However, when I_{ratio} is 6.4, the maximum η_G is only 71.6% in the case of Gaussian beam, which is much smaller than the maximum photon conversion

efficiency of the plane wave approximation. This is because that the intensity distribution of Gaussian beam is not uniform in the cross section compared with the plane wave, which results in non-uniform distribution of the photon conversion efficiency, and further results in the decline of photon conversion efficiency.

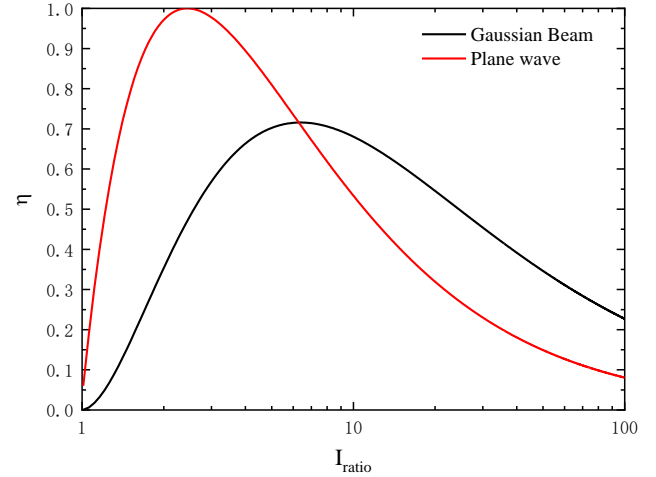


Fig. 2. The plot of the photon conversion efficiency of singly resonant OPO as a function of the intensity ratio I_{ratio} under the plane wave approximation and Gaussian beam conditions (color online)

3.2. Analysis of the relationship between cavity-enhanced photon conversion efficiency, incident power ratio and reflectivity of input coupler based on pump-enhanced singly resonant OPO

To improve the photon conversion efficiency of pump Gaussian beam, pump-enhanced singly resonant OPO can be used. In numerical simulation, the reflectivity of output coupler M2 is 98.5% at 1.4 μ m signal wave and the reflectivity of the other cavity mirrors at 1.4 μ m is 99.8%, the reflectivity of cavity mirrors (excluding the input coupler M3) is 99.8% at 1.064 μ m pump wave, the linear loss of nonlinear crystal for the pump is 0.3%, so $\delta_p = 0.9\%$. The reflectivity of input coupler M3 at 1.064 μ m should be optimized so as to fulfill the condition of impedance matching.

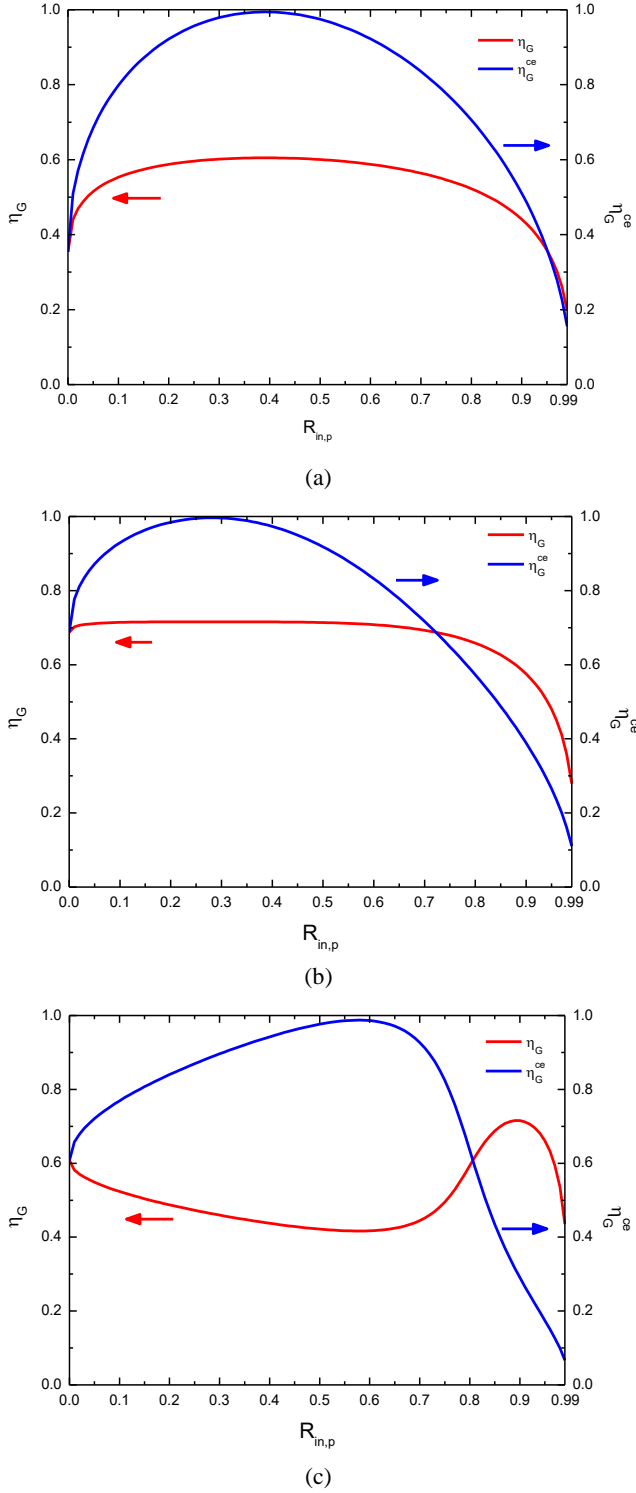


Fig. 3. Simulation of intracavity photon conversion efficiency η_G (red curve) and cavity-enhanced photon conversion efficiency η_G^{ce} (blue curve) as functions of the reflectivity of input coupler $R_{in,p}$ when the incident power ratio $P_{ratio}^{in,p}$ is (a) 2, (b) 4.5, (c) 15, respectively (color online)

By solving Eqs. (12), (13), (15) and (18), the intracavity photon conversion efficiency η_G and the

cavity-enhanced photon conversion efficiency η_G^{ce} as functions of the reflectivity of input coupler $R_{in,p}$ and the incident power ratio $P_{ratio}^{in,p}$ can be obtained. Fig. 3 shows variation curves of η_G and η_G^{ce} with $R_{in,p}$ when the incident power ratio $P_{ratio}^{in,p}$ is (a) 2, (b) 4.5, (c) 15, respectively. The results indicate that the cavity-enhanced photon conversion efficiency η_G^{ce} gradually increases first and then decreases with the increase of $R_{in,p}$. In Fig. 3(a), $P_{ratio}^{in,p}$ is 2, the maximum value 99.4% of η_G^{ce} is expected at the optimum coupling $R_{in,p} = 39\%$, the corresponding η_G is 0.60. In Fig. 3(b), $P_{ratio}^{in,p}$ is 4.5, the maximum value 99.6% of η_G^{ce} is expected at the optimum coupling $R_{in,p} = 28\%$, the corresponding η_G is 0.72. In Fig. 3(c), $P_{ratio}^{in,p}$ is 15, the maximum value 98.8% of η_G^{ce} is expected at the optimum coupling $R_{in,p} = 58\%$, the corresponding η_G is 0.42. The above three examples illustrate the condition for maximum η_G^{ce} is that η_G is approximately equal to $R_{in,p}$ which can be seen as an impedance matching condition. Moreover, when $R_{in,p}$ exceeds the optimum, the pump is undercoupled, η_G^{ce} decreases much faster than it does in the overcoupled regime where reflectivity is lower than the optimum. In addition, in Fig. 3(a)-(b), with the increase of $R_{in,p}$, the intracavity photon conversion efficiency η_G changes very slowly first and then decreases for a low $P_{ratio}^{in,p}$. However, for a high $P_{ratio}^{in,p}$, in Fig. 3(c), the intracavity photon conversion efficiency η_G shows a trend with first a decreasing, then an increasing, and then a decreasing dependence on $R_{in,p}$. The reason for this variation is that the effect of the enhancement factor E_p on the intracavity photon conversion efficiency is not obvious when $P_{ratio}^{in,p}$ is lower, however, for a high $P_{ratio}^{in,p}$, as $R_{in,p}$ increases, the system gradually inclines to impedance matching condition and E_p gradually increase, resulting in an excessive power ratio in the cavity, thereby reducing the intracavity photon conversion efficiency. When $R_{in,p}$ continues to increase, which would yield an under-coupling condition, E_p gradually decreases and the intracavity power ratio tends to the optimum value, so the intracavity photon conversion efficiency increases, later, the intracavity power ratio gradually moves away from the optimum value, the intracavity photon conversion efficiency decreases again.

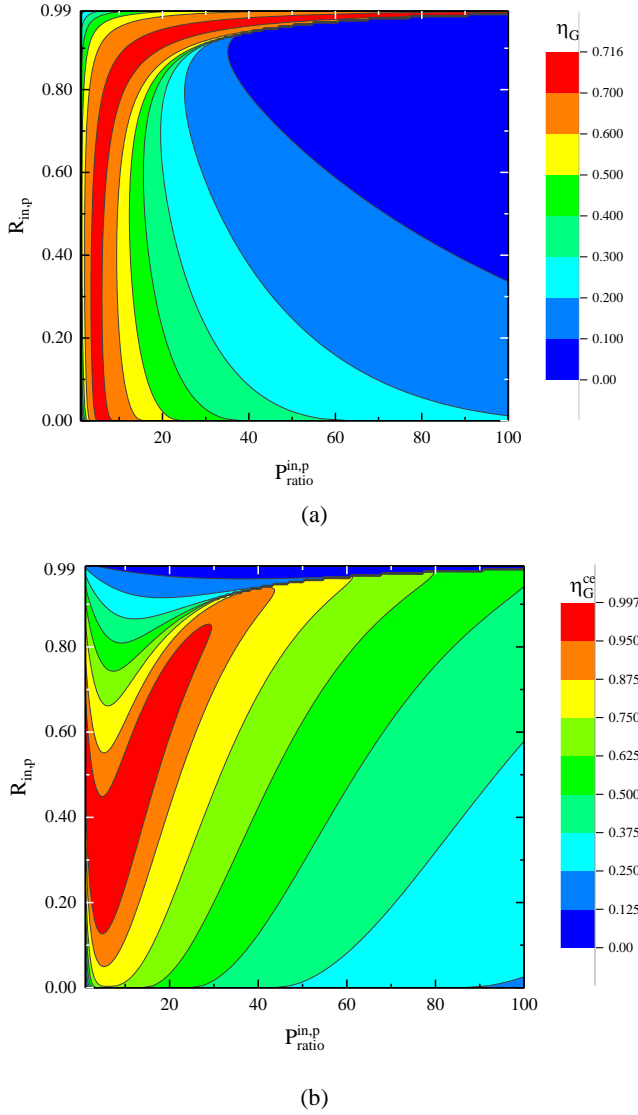


Fig. 4. Contour plots of intracavity photon conversion efficiency η_G (a) and cavity-enhanced photon conversion efficiency η_G^{ce} (b) as functions of the reflectivity of input coupler $R_{in,p}$ and the incident power ratio $P_{ratio}^{in,p}$ under Gaussian beam condition (color online)

Fig. 4(a) shows a contour plot of η_G as a function of $R_{in,p}$ and $P_{ratio}^{in,p}$. When $R_{in,p}$ is constant, the intracavity photon conversion efficiency η_G shows a trend with first an increasing and then a decreasing as the increase of $P_{ratio}^{in,p}$, which is consistent with the conclusion drawn in Fig. 2. The high photon conversion efficiency over 70% can be achieved in the red region, and the maximum of η_G is 71.6%. Considering the cavity-enhanced effect of pump, as $R_{in,p}$ increases, the high-efficiency conversion region is first located in the region where $P_{ratio}^{in,p}$ is about 3.5-8. When $R_{in,p}$ is

increased to 80%, the high-efficiency conversion region begins to extend obviously to the region where $P_{ratio}^{in,p}$ is higher until $P_{ratio}^{in,p}$ is about 46.5, the corresponding $R_{in,p}$ reaches about 97%, and the area gradually becomes very narrow. Fig. 4(b) shows a contour plot of η_G^{ce} as a function of $R_{in,p}$ and $P_{ratio}^{in,p}$. It can be seen from this figure, when $R_{in,p}$ is 0, the relationship between η_G^{ce} and $P_{ratio}^{in,p}$ accords with the conclusion of singly resonant OPO in Fig. 2. The area where η_G^{ce} is more than 95% is called the high-efficiency conversion region (the red region). As $P_{ratio}^{in,p}$ increases, the high-efficiency conversion region moves toward the lower reflectivity first, when $P_{ratio}^{in,p}$ is larger than 4.5, the high-efficiency conversion region moves toward the direction of high reflectivity until $R_{in,p}$ is close to 84%, the corresponding $P_{ratio}^{in,p}$ is 29. This variation law is due to the conclusion that the intracavity photon conversion efficiency η_G has a trend with first an increasing and then a decreasing dependence on $P_{ratio}^{in,p}$. In order to meet the impedance matching, the optimal $R_{in,p}$ first decreases and then increases with the increase of $P_{ratio}^{in,p}$. Therefore, the high-efficiency conversion region basically corresponds to the region of impedance matching, and impedance matching is a necessary condition for high-efficiency conversion. Moreover, the maximum value of η_G^{ce} is 99.6% when $P_{ratio}^{in,p}$ is 4.5, after that, as $P_{ratio}^{in,p}$ increases again, the maximum value of η_G^{ce} will gradually decrease. The pump-enhanced photon conversion efficiency is less than 100%, which is led by the linear loss δ_p of the pump in the cavity.

3.3. Comparison of extraction efficiency between singly resonant OPO and pump-enhanced singly resonant OPO

For singly resonant OPO, the maximum photon conversion efficiency η_G is 71.6%. Considering the linear loss of signal in the ring cavity, the escape efficiency of the ring cavity $\eta_{es} = 68.2\%$. According to Eq. (20), the maximum extraction efficiency of the signal $\eta_{out,s}$ is 48.8%. Since the idler is non-resonant, if the transmittance of output coupler M4 for the idler is 99.8%, the maximum extraction efficiency of the idler $\eta_{out,i}$ is about 71.5% obtained according to Eq. (23).

For pump-enhanced singly resonant OPO, the variation of signal extraction efficiency $\eta_{out,s}^{ce}$ and idler extraction efficiency $\eta_{out,i}^{ce}$ with $R_{in,p}$ and $P_{ratio}^{in,p}$ is consistent with cavity-enhanced photon conversion

efficiency η_G^{ce} as shown in Fig. 4(b). Considering the signal escape efficiency η_{es} of 68.2% and the maximum pump-enhanced photon conversion efficiency η_G^{ce} of 99.6%, the maximum extraction efficiency of the signal $\eta_{out,s}^{ce}$ is 67.9% obtained according to Eq. (21). Considering the transmittance of output coupler M4 for the idler is 99.8%, the maximum extraction efficiency of the idler $\eta_{out,i}^{ce}$ is about 99.4% obtained according to Eq. (24). Through the above comparative analysis, we find that the pump-enhanced singly resonant OPO can effectively improve the photon conversion efficiency of the pump, thereby further improving the extraction efficiency of the signal and idler.

In the case of pump-enhanced singly resonant OPO, by solving the Eqs. (12)-(13), (15) and (19), the contour plots of signal output power $P_{out,s}$ as functions of $R_{in,p}$ and $P_{ratio}^{in,p}$ can be obtained, as shown in Fig. 5. It can be seen from this figure, when $R_{in,p}$ is constant, $P_{out,s}$ increases with the increase of $P_{ratio}^{in,p}$. When $P_{ratio}^{in,p}$ is constant, the variation of $P_{out,s}$ with the increase of $R_{in,p}$ are consistent with that of η_G^{ce} in Fig. 4(b). The idler output power $P_{out,i}$ as functions of $R_{in,p}$ and $P_{ratio}^{in,p}$ has the same changing law as the signal output power $P_{out,s}$, which can be obtained according to Eqs. (16)-(17), (19) and (22). Therefore, the maximum signal and idler output power can be realized based on higher incident power ratio and higher reflectivity of input coupler. During the simulation, the maximum signal output power of 19.1 W and idler output power of 10.9 W can be achieved when $P_{ratio}^{in,p}$ is 100 and the corresponding $R_{in,p}$ is 98%.

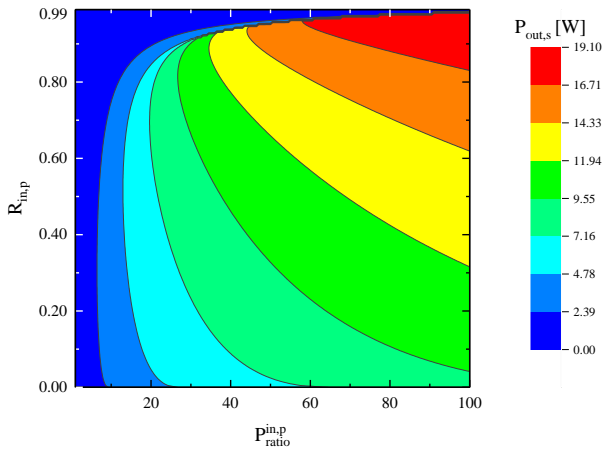


Fig. 5. Contour plots of signal output power $P_{out,s}$ as functions of the reflectivity of input coupler $R_{in,p}$ and the incident power ratio $P_{ratio}^{in,p}$ in the case of pump-enhanced singly resonant OPO (color online)

4. Conclusion

In this paper, we have developed a theoretical treatment that characterizes pump-enhanced singly resonant OPO where both pump and signal simultaneously resonate in the cavity with a MgO:PPLN crystal. In the case of Gaussian beam, the variations of parameters including intracavity photon conversion efficiency, cavity-enhanced photon conversion efficiency, signal and idler extraction efficiency, signal and idler output power with the changes of the reflectivity of input coupler and incident power ratio are analyzed. The study shows that the maximum photon conversion efficiency of pump-enhanced singly resonant OPO can be obtained in the region where the impedance matching is met when the incident power ratio is determined. As incident power ratio increases, the high-efficiency conversion region of more than 95% moves toward the lower reflectivity first, when incident power ratio is larger than 4.5, the high-efficiency conversion region moves toward the direction of high reflectivity. Considering the pump linear loss of 0.9% in the ring cavity, the maximum value of η_G^{ce} is 99.6% when incident power ratio is 4.5.

On the other hand, the maximum signal and idler extraction efficiency of pump-enhanced singly resonant OPO are respectively 67.9% and 99.4%, which are higher than singly resonant OPO where signal and idler extraction efficiency are respectively 48.8% and 71.5%. Whether singly resonant OPO or pump-enhanced singly resonant OPO, to further improve the extraction efficiency of resonant signal, it is necessary to make the linear loss of OPO cavity for the signal much less than the transmittance of the signal output coupler. The idler extraction efficiency is much greater than the resonant signal extraction efficiency, so the band required in actual applications should be set to non-resonant.

The signal and idler output power increase with the rise of the incident power ratio. The maximum signal output power of 19.1 W and idler output power of 10.9 W can be achieved during simulation when the incident power ratio is 100 and the corresponding reflectivity of input coupler is 98%. The conclusions of this paper will provide some guidance for the experiment of pump-enhanced singly resonant OPO.

Acknowledgments

This work was supported by the National Natural Science Foundation of China (Grants 11704236, 11804192).

References

- [1] U. Panne, Trends Anal. Chem. **17**, 491 (1998).
- [2] A. Vogel, B. Kersten, I. Apitz, Proc. SPIE **4961**, 40 (2003).

- [3] F. Lu, M. Z. Jin, M. A. Belkin, *Nature Photon.* **8**, 307 (2014).
- [4] H. H. P. T. Bekman, J. C. Van den Heuvel, F. J. M. van Putten, H. M. A. Schleijsen, *Proc. SPIE* **5615**, 27 (2005).
- [5] A. Soibel, M. W. Wright, W. H. Farr, S. A. Keo, C. J. Hill, R. Q. Yang, H. C. Liu, *IEEE Photonic. Tech. L.* **22**, 121 (2010).
- [6] L. Wang, T. L. Xing, S. W. Hu, X. Y. Wu, H. X. Wu, J. Y. Wang, H. H. Jiang, *Opt. Express* **25**, 3373 (2017).
- [7] J. P. Qiao, S. Z. Zhao, K. J. Yang, J. Zhao, G. Q. Li, D. C. Li, T. Li, W. C. Qiao, *Appl. Phys. B* **123**, 1 (2017).
- [8] V. Ulvila, M. Vainio, *Opt. Commun.* **439**, 99 (2019).
- [9] Q. Liu, J. H. Liu, Z. L. Zhang, M. L. Gong, *Laser Phys. Lett.* **10**, 75407 (2013).
- [10] Y. F. Peng, X. B. Wei, G. Xie, J. R. Gao, D. M. Li, W. M. Wang, *Laser Phys.* **23**, 55405 (2013).
- [11] Y. F. Peng, X. B. Wei, W. M. Wang, D. M. Li, *Opt. Commun.* **283**, 4032 (2010).
- [12] M. Henriksson, M. Tiihonen, V. Pasiskevicius, F. Laurell, *Appl. Phys. B* **88**, 37 (2007).
- [13] J. Q. Zhao, Ph.D. Dissertation, Harbin Institute of Technology 80 (2011).
- [14] P. Li, Y. J. Li, K. S. Zhang, *Laser Phys. Lett.* **12**, 45401 (2015).
- [15] H. B. Jiang, L. F. Shen, Z. G. Zhao, B. Liu, Z. Xiang, D. Liu, C. Liu, *Chinese J. Lasers* **43**, 71 (2016).
- [16] M. K. Shukla, R. Das, *IEEE Journal of Selected Topics in Quantum Electronics* **24**, 1 (2017).
- [17] Sukeert, S. C. Kumar, M. Ebrahim-Zadeh, *Opt. Lett.* **44**, 5796 (2019).
- [18] G. Robertson, M. J. Padgett, M. H. Dunn, *Opt. Lett.* **19**, 21 (1994).
- [19] K. Schneider, P. Kramper, S. Schiller, J. Mlynek, *Opt. Lett.* **22**, 17 (1997).
- [20] D. Chen, D. Hinkley, J. Pyo, J. Swenson, R. Fields, *J. Opt. Soc. Am. B* **15**, 6 (1998).
- [21] U. Strössner, A. Peters, J. Mlynek, S. Schiller, *Opt. Lett.* **24**, 22 (1999).
- [22] S. Schiller, K. Schneider, J. Mlynek, *J. Opt. Soc. Am. B* **16**, 9 (1999).
- [23] G. D. Boyd, D. A. Kleinman, *J. Appl. Phys.* **39**, 3597 (1968).
- [24] W. Tan, X. D. Qiu, G. Zhao, M. Y. Jia, W. G. Ma, X. J. Yan, L. Dong, L. Zhang, Z. M. Tong, W. B. Yin, X. X. Feng, L. T. Xiao, O. Axner, S. T. Jia, *Appl. Phys. B* **123**, 52 (2017).
- [25] X. J. Yan, W. G. Ma, W. Tan, *Acta Phys. Sin.* **65**, 44207 (2016).

*Corresponding author: yanxj@sxu.edu.cn